Constitutive Modelling of Clear Spruce Wood under Biaxial Loading by means of an Orthotropic Single-Surface Model under Consideration of Hardening and Softening Mechanisms

Herbert W. Müllner [1], **Peter Mackenzie-Helnwein** [2], **Josef Eberhardsteiner** [1]

[1] Institute for Strength of Materials, Vienna University of Technology, Vienna, Austria
[2] Civil and Environmental Engineering, University of Washington, Seattle, United States

Abstract

The goal of this contribution is the development of a plane stress orthotropic plasticity material model for clear spruce wood. Such a model has to consider an initially linear elastic domain as well as hardening and softening behaviour at higher states of stress and strain, respectively. Combining the advantage of a smooth single-surface plasticity model with the identification of distinct hardening and softening laws for tension and compression loading in longitudinal and radial direction is the key to the novel mathematical formulation presented in this contribution. By associating characteristic strength values of the single-surface model with the respective characteristic failure modes, one can define a set of nonlinear evolution laws for six parameters of the criterion by TSAI & WU [10]. Such a modification redefines the meaning of the original failure envelope as a yield surface. Depending on the stress state, plastic loading causes hardening or softening. This is represented by changing size and location of the elliptic yield surface in the orthotropic stress space [8]. The verification of the developed model is given for the entire plane stress in the orthotropic stress space by means of back-calculation of the biaxial experiments by EBERHARDSTEINER [3].

1 Introduction

As basis of the suggested material model serves an experimental investigation of the failure envelope for biaxial stressed wood by EBERHARDSTEINER [3]. He described the failure envelope by means of the orthotropic elliptic failure criterion by TSAI & WU [10] which identifies failure states as a boundary of a linear elastic domain. The idea of a single-surface model offers a reasonably simple mathematical description of an orthotropic yield surface by means of six independent material parameters.

By defining characteristic strength values, depending of these six material parameters, MÜLLNER [8] combined these values with micromechanically motivated failure modes identified and applied to a multi-surface plasticity model by MACKENZIE-HELNWEIN et al. [6]. The determination of the material parameters results in a nonlinear equation system. Thus, the advantage of a single-surface model has to be paid for by the extra effort of locally solving these nonlinear equations. Moreover, application of the classical return mapping algorithm of SIMO & HUGHES [9] yields an unsymmetric consistent tangent for this model.

In Chapter 2 of this paper a short description of the used biaxial testing device is given [3]. In Chapter 3 four failure modes of biaxial stressed wood are identified. Chapter 4 refers to the material model. Because of the brittle tensile and the ductile compression behaviour of wood the formulation of a non-associated hardening and softening rule is required. The verification of the material model is given in Chapter 5 by comparing the results of the experiments with the ones of back-calculations by means of the proposed material model. The paper will be completed by conclusions and some present research activities.

2 Experimental investigation of spruce wood under biaxial loading

Constitutive modelling of the biaxial mechanical behaviour of solid wood requires knowledge of both, the stress-strain relations in the pre-failure domain as well as the failure locations for arbitrary strain paths. Both requirements were satisfied in a comprehensive test series carried out by EBERHARDSTEINER [3]. In Fig. 1(a) the used cruciform specimen is shown. With a constant moisture content of u = 12 %, a series of 439 displacement-driven biaxial strength tests were performed. These tests cover the whole set of distinguishable stress states for an orthotropic material under plane stress conditions in the *LR*-plane, where *L* is the longitudinal and *R* is the radial direction within the stem of a tree. The individual tests differ in two mechanical parameters:

- *grain angle* φ – it is the angle between principal loading direction and grain direction.
- *displacement ratio* κ – it is defined as $\kappa = u : v$, with u and v according to Fig. 1(b).

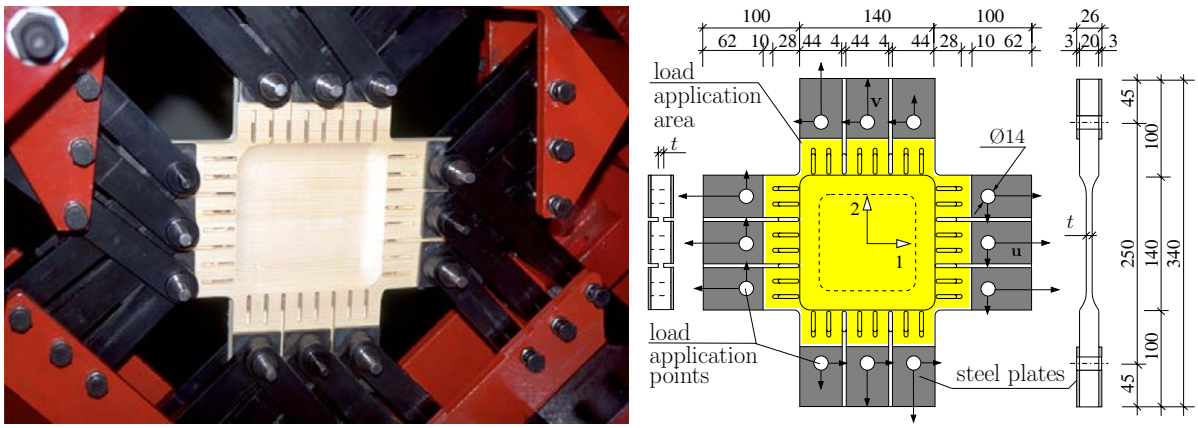

Figure 1 a, b: *Experimental investigation of spruce wood under biaxial loading*
(a) *wooden specimen mounted in the biaxial testing device*
(b) *dimensions in [mm] of the cruciform specimen and applied displacements*

Figure 2 refers to all experiments performed at grain angle of $\varphi = 0°$ and $\varphi = 30°$, respectively. The axis values are the principal stresses, σ_1 and σ_2, which are aligned with the horizontal and vertical axis of the test specimen. Each line represents the stress path obtained from a single test under proportionally increasing prescribed displacements. The symbol at the end of each line indicates the end of the elastic behaviour, which has been defined as the end of the linear part of the different stress ratios.

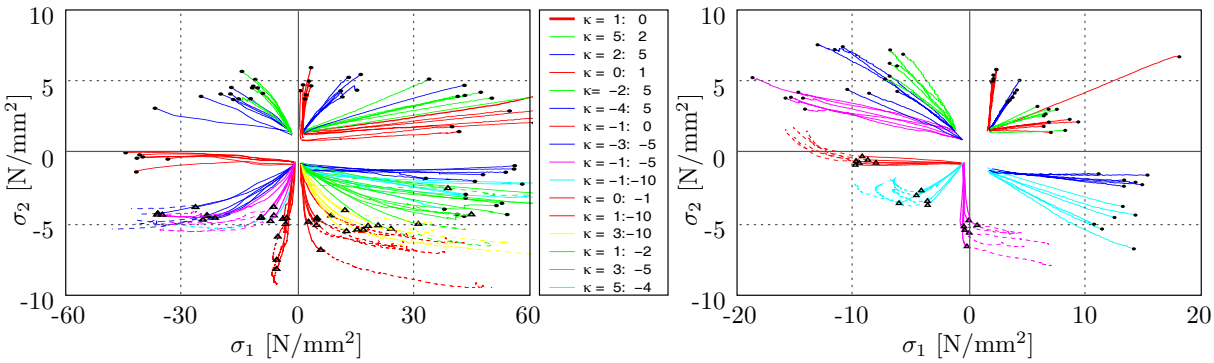

Figure 2 a, b: *Biaxial strength test data and evolution of principal stress ratio* σ_2 / σ_1
(a) *for grain direction* $\varphi = 0°$ *and various displacement ratios* κ
(b) *for grain direction* $\varphi = 30°$ *and various displacement ratios* κ

3 Identification of four basic modes of failure

The obtained failure locations reveal an elliptic shape of the failure envelope. EBERHARD-STEINER [3] described that envelope by means of the orthotropic failure criterion by TSAI & WU [10] which identifies failure states as a boundary of a linear elastic domain. This failure criterion corresponds with a second-order tensor polynomial and is shown in Fig. 3.

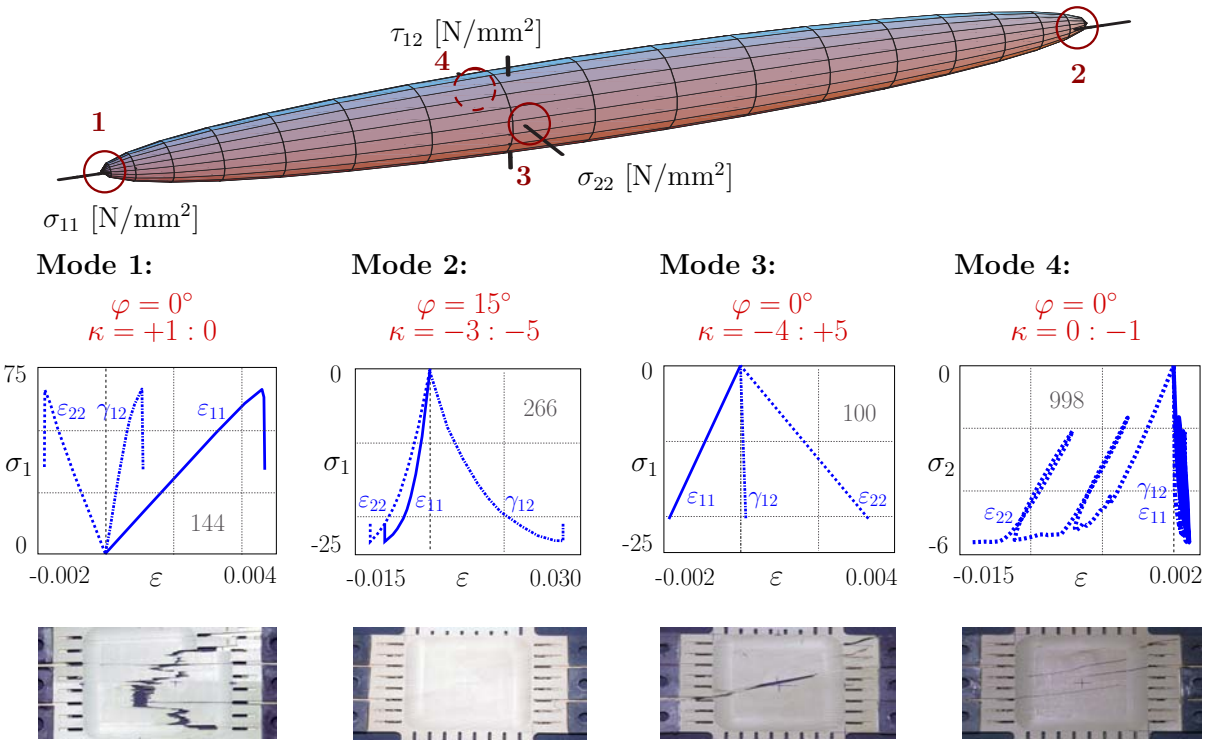

Figure 3: *Elliptic failure envelope by TSAI & WU and characteristic stress-strain curves and fracture types for different biaxial loading situations*

Analyzing the stress-strain relations for different load ratios MACKENZIE-HELNWEIN et al. [6] characterised four modes of failure, illustrated in Fig. 3 with a stress-strain diagram and an image of the specimen at fracture:

- *Mode 1 – Brittle tensile failure in fibre direction:* This mode shows a large variation of strength. The respective cascading crack pattern can only be found for small grain angles.
- *Mode 2 – Compressive failure in fibre direction:* Strength degradation to 70-80 % of the initial failure stress occurs, because bands of damaged cells (kink formation) develop.
- *Mode 3 – Brittle tensile failure perpendicular to grain:* This mode is characterised by a distinct straight crack parallel to grain. It can be found for all grain angles.
- *Mode 4 – Ductile compressive behaviour perpendicular to grain:* Compressive loading exactly perpendicular to grain leads to strength hardening.

At large deformations, both compressive modes 2 and 4, show a phenomenon called *densification*, where the strength rises and the material becomes almost rigid [1].

Typically, single-surface models with associated hardening do not permit the identification of these micromechanical failure modes. Therefore, the formulation of a non-associated hardening or softening rule has to occur, ensuring an appropriate change of the size of the yield surface.

4 Single-surface plasticity model

4.1 Orthotropic invariants for plane stress

Assuming small strains, the following set of stress invariants is used for the mathematical description of orthotropic tensor functions for plane stress in the *LR*-plane [6]:

$$\sigma_L = \operatorname{tr} \boldsymbol{\sigma} \mathbf{M}_L \quad , \qquad \sigma_R = \operatorname{tr} \boldsymbol{\sigma} \mathbf{M}_R \quad , \qquad \tau_{LR}^2 = \operatorname{tr} \boldsymbol{\sigma} \mathbf{M}_R \boldsymbol{\sigma} \mathbf{M}_L \ . \tag{1}$$

Using engineering strain for shear deformations, the strain invariants are similar to (1):

$$\varepsilon_L = \operatorname{tr} \boldsymbol{\varepsilon} \mathbf{M}_L \quad , \qquad \varepsilon_R = \operatorname{tr} \boldsymbol{\varepsilon} \mathbf{M}_R \quad , \qquad \gamma_{LR}^2 = 4 \operatorname{tr} \boldsymbol{\varepsilon} \mathbf{M}_R \boldsymbol{\varepsilon} \mathbf{M}_L \ . \tag{2}$$

The structural tensors $\mathbf{M}_L$, $\mathbf{M}_R$ and $\mathbf{M}_T$ [2] are defined with the unit normal vectors locally aligned with the principal directions of the tree as shown in Fig. 4:

$$\mathbf{M}_L = \mathbf{A}_L \otimes \mathbf{A}_L \qquad \mathbf{M}_R = \mathbf{A}_R \otimes \mathbf{A}_R \qquad \mathbf{M}_T = \mathbf{A}_T \otimes \mathbf{A}_T \tag{3}$$

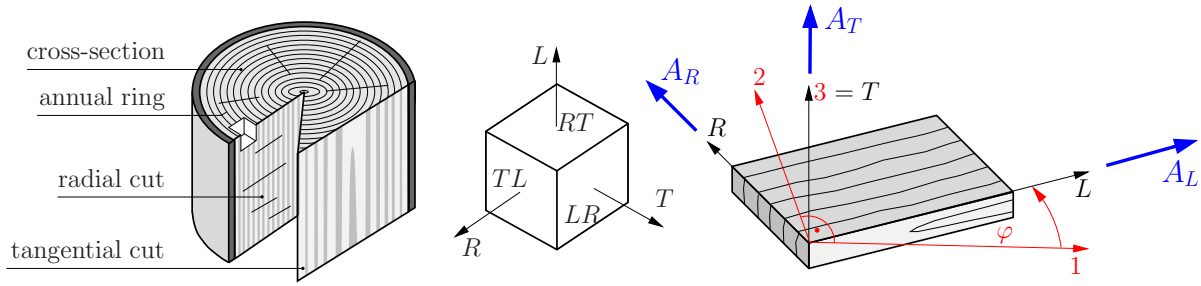

Figure 4: *Material orientation and definition of the unit normal vectors* $\mathbf{A}_L$, $\mathbf{A}_R$ *and* $\mathbf{A}_T$

4.2 Linear elastic orthotropic behaviour

As can be seen from Figs. 2 and 3, wood possesses linear elastic behaviour initially and at unloading phases as well as in the tensile and compressive regime. Hyperelastic behaviour defines the stress as

$$\boldsymbol{\sigma} = \frac{\partial \psi}{\partial \boldsymbol{\varepsilon}} = \mathbb{C} : \left(\boldsymbol{\varepsilon} - \boldsymbol{\varepsilon}^p \right), \tag{4}$$

where $\boldsymbol{\varepsilon}$ denotes the total strain state and $\boldsymbol{\varepsilon}^p$ the plastic strain state. The linear elastic stiffness tensor $\mathbb{C}$ in (4) follows from the standard hyperelastic orthotropic formulation based on a HELMHOLTZ free energy function ψ as

$$\mathbb{C} = \frac{E_L}{\Delta} \mathbf{M}_L \otimes \mathbf{M}_L + \frac{E_R}{\Delta} \mathbf{M}_R \otimes \mathbf{M}_R + \frac{\nu_{LR} E_R}{\Delta} \left(\mathbf{M}_L \otimes \mathbf{M}_R + \mathbf{M}_R \otimes \mathbf{M}_L \right) + G_{LR} \mathbb{M} \, , \tag{5}$$

where E_L, E_R and ν_{LR} are three independent material parameters with $\Delta = 1 - \nu_{LR}^{\ 2} E_R / E_L$. The shear stiffness G_{LR} can be obtained from these independent material parameters by means of the invariance assumption by LEKHNITSKIJ [5] as

$$G_{LR} = \frac{E_L \, E_R}{E_L + E_R + 2 \nu_{LR} E_R} \ . \tag{6}$$

Finally, the structural tensor of fourth order in (5) is defined as

$$\mathbb{M} = \left(\mathbf{A}_L \otimes \mathbf{A}_R + \mathbf{A}_R \otimes \mathbf{A}_L \right) \otimes \left(\mathbf{A}_L \otimes \mathbf{A}_R + \mathbf{A}_R \otimes \mathbf{A}_L \right) \ . \tag{7}$$

4.3 Orthotropic yield surface and failure envelope

The idea of a single-surface model offers a reasonably simple mathematical description of an orthotropic yield surface by means of six independent material parameters for plane stress states in the *LR*-plane. The basis of the single-surface description is the elliptic yield condition by TSAI & WU [10]

$$f(\boldsymbol{\sigma},\mathbf{p}) = \mathbf{a}(\mathbf{p}):\boldsymbol{\sigma} + \boldsymbol{\sigma}:\mathbf{b}(\mathbf{p}):\boldsymbol{\sigma} - 1 = 0 \ , \tag{8}$$

where **a** and **b** are variable orthotropic tensors of second and fourth order, respectively. They are defined as

$$\mathbf{a} = a_{LL}\,\mathbf{M}_L + a_{RR}\,\mathbf{M}_R \quad \text{and} \tag{9a}$$

$$\mathbf{b} = b_{LLLL}\,\mathbf{M}_L \otimes \mathbf{M}_L + b_{RRRR}\,\mathbf{M}_R \otimes \mathbf{M}_R + b_{LLRR}\left(\mathbf{M}_L \otimes \mathbf{M}_R + \mathbf{M}_R \otimes \mathbf{M}_L\right) + b_{LRLR}\,\mathbb{M} \ . \tag{9b}$$

Because of the orthotropic characteristics of wood and the restriction to plane stress states, only six independent material parameters are required to describe **a** and **b**. These parameters which define a yield surface for clear spruce wood in orthotropic stress space are collected in the vector

$$\mathbf{p} = \lfloor a_{LL} \quad a_{RR} \quad b_{LLLL} \quad b_{RRRR} \quad b_{LLRR} \quad b_{LRLR} \rfloor^T \ . \tag{10}$$

MÜLLNER [8] determined the values of these material parameters as:

$$\mathbf{p} = \lfloor -0.004725 \quad -0.030672 \quad +0.000309 \quad +0.054853 \quad +0.000382 \quad +0.003452 \rfloor^T \ , \tag{11}$$

where the dimension of the coefficients a_{ij} is [mm²/N] and of the coefficients b_{ijkl} it is [mm⁴/N²] ($i, j, k, l = \{L, R\}$). The determined yield surface is shown in Fig. 5.

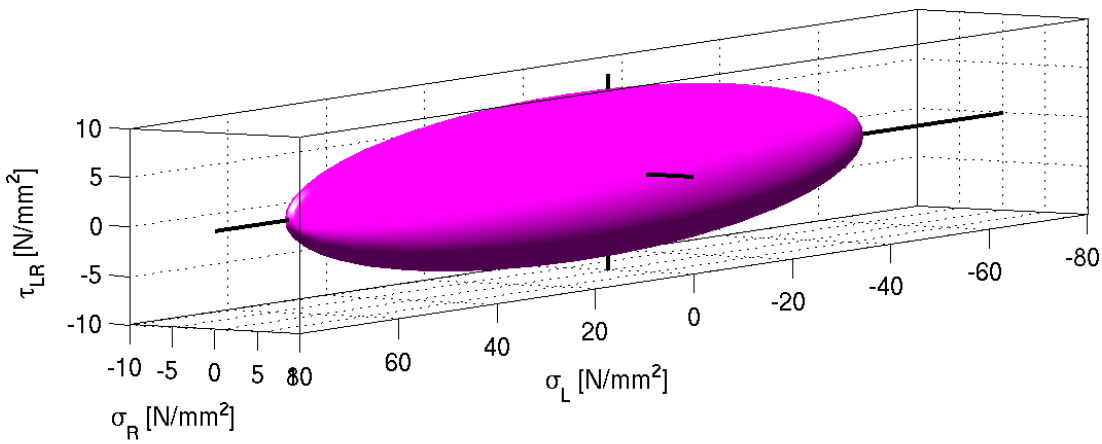

Figure 5: *Yield surface of single-surface material model in the orthotropic stress space*

4.4 Associated flow rule – evolution law for plastic strain

The evolution law for the plastic strains can be described by means of a flow potential formulation by SIMO & HUGHES [9]. Under consideration of *associated plasticity* the flow rule reduces to

$$\dot{\boldsymbol{\varepsilon}}^p = \dot{\gamma}\frac{\partial f}{\partial \boldsymbol{\sigma}} = \dot{\gamma}\left(\mathbf{a} + 2\,\mathbf{b}\,\boldsymbol{\sigma}\right) = \dot{\gamma}\,\mathbf{r} \ , \tag{12}$$

with $\dot{\gamma}$ as a proportionality factor, the so-called consistency parameter.

4.5 Non-associated hardening and softening rule – evolution law for primary variables

The five maxima of the strength values, $max\,\beta_{i,j}$ ($i = \{t,c\}$, $j = \{L,R\}$) as well as $max\,\tau_{LR}$, and the inclination $tan\,\phi^*$ of the yield surface in the plane $\tau_{LR} = 0$ shown in Fig. 6(a) and (b) will be formulated as functions of the six components of the vector **p**.

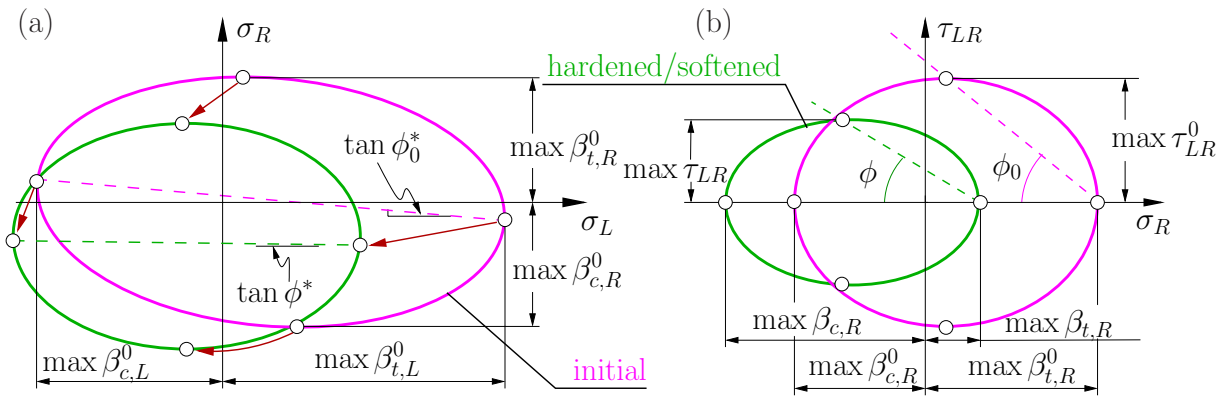

Figure 6 a, b: *Characteristic strength values of the single-surface model*
(a) *tensile and compressive strength in the plane* $\tau_{LR} = 0$
(b) *tensile and compressive strength in R-direction and maximal shear strength*

These six values are on the one hand controlled by the vector **p** of (10) and on the other hand multiplied by the evolution laws. With these two definitions a residual vector

$$\mathbf{R} = \begin{Bmatrix} \max\beta_{t,L}(\mathbf{p}) \\ \max\beta_{c,L}(\mathbf{p}) \\ \max\beta_{t,R}(\mathbf{p}) \\ \max\beta_{c,R}(\mathbf{p}) \\ \tan\phi^*(\mathbf{p}) \\ \max\tau_{LR}(\mathbf{p}) \end{Bmatrix} - \begin{Bmatrix} \max\beta_{t,L}^0\, e^{-k_{t,L}\,\alpha_{t,L}} \\ \max\beta_{c,L}^0 - Y_{1,L}\,(1-e^{-k_{c,L}\,\alpha_{c,L}}) + q_L(\alpha_{c,L}) \\ \max\beta_{t,R}^0\, e^{-k_{t,R}\,\alpha_{t,R}} \\ \max\beta_{c,R}^0 + Y_{1,R}\,(1-e^{-k_{c,R}\,\alpha_{c,R}}) + q_R(\alpha_{c,R}) \\ \tan\phi_0^*\, e^{-k_{t,R}\,\alpha_{ref}} \\ \dfrac{\max\beta_{t,R}\,(\alpha_{t,R}) + \max\beta_{c,R}\,(\alpha_{c,R})}{2}\tan[\phi_\infty + (\phi_0 - \phi_\infty)\, e^{-k_{shr}\,\alpha_{shr}}] \end{Bmatrix} = \mathbf{0} \quad (13)$$

can be defined as shown in (13). If plastic strains occur, the residual **R** is not satisfied and the components of the vector **p** have to be modified. The obtained nonlinear equation system is solved by means of the NEWTON-RAPHSON-method. The new entries of **p** define a new yield surface without changing the mathematical form of (8).

Different evolution laws implicate different hardening or softening rules, respectively. Thus, the non-associated hardening or softening rule for the single-surface model results as

$$\dot{\boldsymbol{\alpha}} = \begin{Bmatrix} \alpha_{t,L} \\ \alpha_{c,L} \\ \alpha_{t,R} \\ \alpha_{c,R} \\ \alpha_{ref} \\ \alpha_{shr} \end{Bmatrix} = \dot{\gamma} \begin{Bmatrix} \langle\ \mathbf{M}_L : \mathbf{r}\rangle \\ \langle -\mathbf{M}_L : \mathbf{r}\rangle \\ \langle\ \mathbf{M}_R : \mathbf{r}\rangle \\ \langle -\mathbf{M}_R : \mathbf{r}\rangle \\ \langle\ \mathbf{M}_R : \mathbf{r}\rangle \\ 2\left|\sqrt{\mathrm{tr}\,\mathbf{M}_R\,\mathbf{r}\,\mathbf{M}_L\,\mathbf{r}}\right| \end{Bmatrix} = \dot{\gamma}\,\mathbf{s}\ . \quad (14)$$

5 Results and verification of the developed material model for clear spruce wood

Figure 7 shows as an example the initial and the modified yield surface in case of plastic deformations due to tension loading in fibre direction. As explained in Chapter 3 this kind of load is connected with a cascading crack pattern. In the case of alternating loading the material accepts compression loading despite of the crack.

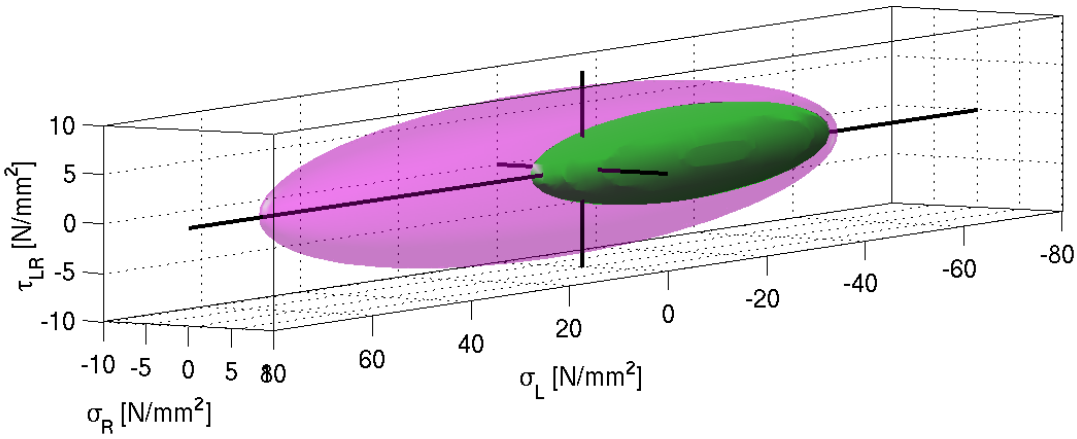

Figure 7: *Initial (magenta) and modified (green) yield surface for softening in L-direction*

The verification of the developed model is given for the entire plane stress orthotropic stress space by means of back-calculation of the biaxial experiments by EBERHARDSTEINER [3]. For the present calculations, a proportional strain path based on ideal test parameters was considered, by equating the ratio $\kappa = u : v$ with the strain-ratio $\varepsilon_1 : \varepsilon_2$, where ε_1 and ε_2 are strain components according to Fig. 1(b). Doing so, the failure diagrams of [3] were simulated (Two examples are shown in Fig. 2.). The performed simulations of the mentioned experiments (Fig. 8) show a good agreement between the model and the test results for most modes of biaxial loading. Similar diagrams for grain angles of $\varphi = 7.5°$, 15°, and 45° were performed by MÜLLNER [8]. Minor deviations are a consequence of restricting the yield condition to an elliptical surface. However, the obtained results are superior to any method suggested by design codes.

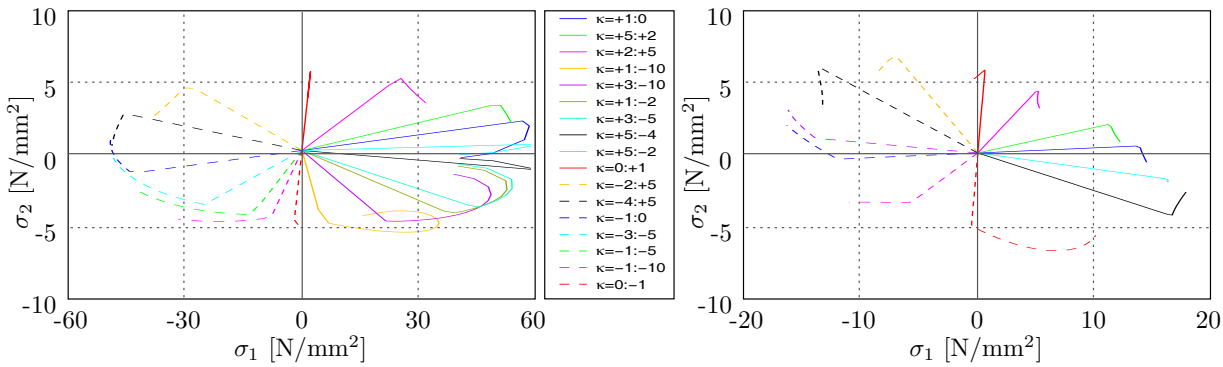

Figure 8 a, b: *Results of the simulation of the experiments and evolution of stress ratio σ_2 / σ_1*
(a) *for grain direction $\varphi = 0°$ and various displacement ratios κ*
(b) *for grain direction $\varphi = 30°$ and various displacement ratios κ*

The comparison of experimental and numerical obtained results shows that the single-surface plasticity model with non-associated hardening and softening rules and the presented material parameters are a good tool to describe the mechanical behaviour of clear spruce wood.

6 Conclusions and present research activities

A new constitutive model for the simulation of clear spruce wood under biaxial states of plane stress has been presented. It is based on observations from a comprehensive test series for the experimental identification of the failure envelope for clear spruce wood under arbitrary biaxial stress states. Employing this as well as microscopic observations and their macroscopic translation led to the multi-surface plasticity model by MACKENZIE-HELNWEIN et al. [6]. It consists of four surfaces representing four basic failure modes. The separated description of four modes easily enables the modelling of their respective post-failure behaviour.

The more extensive mechanical description inherits the extra mathematical and computational effort for the treatment of edge and corner problems. This leads to the intention to combine the prediction of failure modes with the simplicity of a smooth single-surface model. It can be achieved by tracing a series of strain-type variables, each representing one of the previously introduced scalar hardening and softening parameters.

In order to simulate real structures and other examples of practical relevance the presented material model will be implemented in a Finite Element program. Furthermore, the effect of transverse shear for the analysis of shear-deformable shells made of wood is considered by MACKENZIE-HELNWEIN et al. [7]. In addition, the effect of knots and the respective fibre deviations to the various strength values is investigated by FLEISCHMANN et al. [4].

References

1. Adalian C., Morlier P. (2002): “Wood Model” for the Dynamic Behaviour of Wood in Multiaxial Compression. Holz als Roh- und Werkstoff, 60 (6): 433-439.
2. Betten J. (1987): Applications of Tensor Functions in Solid Mechanics. CISM courses and lectures, 292: Chapter 11-14.
3. Eberhardsteiner J. (2002): Mechanisches Verhalten von Fichtenholz – Experimentelle Bestimmung der biaxialen Festigkeitseigenschaften. Springer, Vienna, in German.
4. Fleischmann M., Eberhardsteiner J., Ondris L. (2003): Experimental Investigation of Spruce Wood in Different Material Directions and Constitutive Modelling Including Knot Effects. 20th Danubia-Adria Symposium on Experimental Methods in Solid Mechanics – Abstracts: 14-15.
5. Lekhnitskij S.G. (1981): Theory of Elasticity of an Anisotropic Body. Mir Publishers, Moscow.
6. Mackenzie-Helnwein P., Eberhardsteiner J., Mang H.A. (2003): A Multi-Surface Plasticity Model for Clear Wood and its Application to the Finite Element Analysis of Structural Details. Computational Mechanics, 31 (1-2): 204-218.
7. Mackenzie-Helnwein P., Müllner H.W., Eberhardsteiner J., Mang, H.A. (2004): Analysis of Layered Wooden Shells using an Orthotropic Elasto-Plastic Model for Multiaxial Loading of Clear Spruce Wood. Computer Methods in Applied Mechanics and Engineering, in print.
8. Müllner H.W. (2003): Konstitutives Modellieren von Fichtenholz unter biaxialer Beanspruchung mittels eines orthotropen Einflächenmodells unter Berücksichtigung von Ver- und Entfestigung. Master’s Thesis, Vienna University of Technology, in German.
9. Simo J.C., Hughes T.J.R. (1998): Computational Inelasticity – Interdisciplinary Applied Mathematics, Springer, New York.
10. Tsai S.M., Wu E.M. (1971): A General Theory of Strength for Anisotropic Materials. Journal of Composite Materials, 5: 58-80.